J|A|C|S
ARTICLES
Published on Web 05/24/2002

Hydrogen Activation on Mo-Based Sulfide Catalysts, a Periodic DFT Study

Arnaud Travert,*,† Hiroyuki Nakamura,†,§ Rutger A. van Santen,† Sylvain Cristol,‡,|| Jean-François Paul,‡ and Edmond Payen‡

Contribution from the Schuit Institute of Catalysis, Laboratory of Inorganic Chemistry and Catalysis, Eindhoven University of Technology, P.O. Box 513, 5600 MB Eindhoven, The Netherlands, and Laboratoire de Catalyse, UPRESA CNRS 8010, bât. C3, Université des Sciences et Technologies de Lille, 59650 Villeneuve d'Ascq Cedex, France

Received July 5, 2001

Abstract: Hydrogen adsorption on Mo−S, Co−Mo−S, and Ni−Mo−S ($10\bar{1}0$) surfaces has been modeled by means of periodic DFT calculations taking into account the gaseous surrounding of these catalysts in working conditions. On the stable Mo−S surface, only six-fold coordinated Mo cations are present, whereas substitution by Co or Ni leads to the creation of stable coordinatively unsaturated sites. On the stable MoS_2 surface, hydrogen dissociation is always endothermic and presents a high activation barrier. On Co−Mo−S surfaces, the ability to dissociate H_2 depends on the nature of the metal atom and the sulfur coordination environment. As an adsorption center, Co strongly favors molecular hydrogen activation as compared to the Mo atoms. Co also increases the ability of its sulfur atom ligands to bind hydrogen. Investigation of surface acidity using ammonia as a probe molecule confirms the crucial role of sulfur basicity on hydrogen activation on these surfaces. As a result, Co−Mo−S surfaces present Co−S sites for which the dissociation of hydrogen is exothermic and weakly activated. On Ni−Mo−S surfaces, Ni−S pairs are not stable and do not provide for an efficient way for hydrogen activation. These theoretical results are in good agreement with recent experimental studies of H_2−D_2 exchange reactions.

1. Introduction

Hydrotreating covers a variety of catalytic hydrogenation processes that aim at reducing the heteroatom content of petroleum feedstocks.[1] More stringent environmental regulations have urged refiners on the improvement of the hydrodesulfurization processes, one possible approach being the development of better catalysts. The vast majority of hydrotreating catalysts used nowadays consists of mixed CoMo or NiMo sulfides highly dispersed on high surface area carriers such as alumina. It is well known that both mixed sulfides exhibit a much higher activity (1 order of magnitude) than the corresponding monometallic Mo catalysts, an increase which is often referred to as the *promoting effect* of Co or Ni on Mo-based catalysts. Despite the intense research effort in the domain during the past decades, the molecular basis of the promoting effect is still controversial.

Under the hydrotreating reaction conditions, the thermodynamically stable monometallic Mo sulfide phase is molybdenite,[2] the structure of which consists of the stacking of MoS_2 sheets of hexagonal symmetry.[3] It is generally concluded that the active phase of supported Mo catalysts is similar and consists of small MoS_2 particles (few nanometers), whose active sites are coordinatively unsaturated (CUS) molybdenum atoms located at the edge of MoS_2 crystallites. On this basis, several models have been proposed that explain the synergetic effect between Co (Ni) and Mo.

Thus, in the "remote-control" model, Delmon et al.[4] have considered the existence of two distinct sulfide phases on the working catalyst. The sulfide phase which is formed by the promoter (e.g., Co_9S_8) would activate hydrogen which would then spill-over toward the MoS_2 phase, that would maintain a fraction of surface Mo in coordinative unsaturation (active for hydrogenation) and form −SH groups that would be active for hydrogenolysis.

On the other hand, the existence of a direct contact between Co (Ni) sulfide species and MoS_2 has been demonstrated by many spectroscopic techniques.[5−8] The question that arised from

* To whom correspondence should be addressed. Phone: +33 (0)2 31 45 28 23. Fax: +33 (0)2 31 45 28 22. E-mail: arnaud.travert@ismra.fr.
† Schuit Institute of Catalysis.
‡ Laboratoire de Catalyse.
§ Permanent address: Japan Energy Corp., 3-17-35, Niizominami, Todashi, Saitama 335-8502, Japan.
|| Present address: The Royal Institution of Great Britain, 21 Albermale Street, London W1S 4BS, United Kingdom.

(1) Topsøe, H.; Clausen, B. S.; Massoth, F. E. In *Hydrotreating Catalysis, Science, and Technology*; Anderson, J. R., Boudard, M., Eds.; Springer-Verlag: Berlin/New York, 1996.
(2) Furimsky, E. *Catal. Rev.-Sci. Eng.* **1980**, *22*, 371.
(3) Bronsema, K. D.; de Boer, J. L.; Jellinek, F. *Z. Anorg. Allg. Chem.* **1986**, *15*, 540.
(4) (a) Delmon, B. *Bull. Soc. Chim. Belg.* **1979**, *88*, 979. (b) Delmon, B. In *Catalysts in Petroleum Refining 1989*; Trimm, D. L., Akashah, S., Absi-Halabi, M., Bishara, A., Eds.; Elsevier: Amsterdam, 1990; p 1. (c) Delmon, B. *Catal. Lett.* **1993**, *22*, 1. (d) Li, Y. W.; Delmon, B. *J. Mol. Catal. A: Chem.* **1997**, *127*, 163.
(5) Topsøe, H.; Clausen, B. S.; Lengeler, B.; Candia, R.; Wivel, C.; Morup, S. *J. Catal.* **1981**, *68*, 433.

10.1021/ja011634o CCC: $22.00

these experimental studies is whether the active sites resulting from this contact belong to Co or Mo species.

By measuring the intrinsic HDS activity of highly dispersed Co/C and CoMo/C catalysts, Vissers et al. did not observe significant activity differences between both catalysts.[9] This finding led the authors to propose a dispersion model where MoS_2 would act as a secondary support for Co sulfide particles that would be active by themselves. More recently, however, new HDS activity measurements together with H_2-D_2 exchange experiments carried out on similar systems have made this model questionable.[10]

By now, it is generally believed that the promotor effect results essentially from specific modifications of the MoS_2 surface induced by the promotor. The precise origin of the promoting effect, however, is still not understood insofar as promoted systems do not form a phase in the crystallographic sense, and little is known about their structures at the molecular scale; usual spectroscopic techniques only give indirect information, whereas the very first surface science studies of these materials have only appeared recently.[11] On the other hand, recent developments in periodic density functional theory (DFT) calculations have recently made possible realistic theoretical investigations of these systems.[12−21] Technical aspects of these calculations will be discussed in the next section.

The first periodical DFT calculations on Mo-based sulfide catalysts were carried out by Byskov et al.[12−14] Thus, using Mo_2S_4 chains as a model for unpromoted Mo catalysts, they could show that substitution of Mo by promotor atoms such as Co or Ni leads to a significant decrease of the binding energies of exposed sulfur atoms and leads to the creation of stable sulfur vacancies.[13] More recently, using a larger model, Raybaud et al. have performed a thorough study of the structure of MoS_2 surfaces[15,16] and promoted Mo catalysts.[17] The use of a thermodynamical approach to take into account the gaseous H_2S/H_2 surroundings of the working catalysts has made possible the determination of their sulfur coverages.[16−21] Although these last computed surface structures showed important differences with the earlier studies of Byskov et al., the striking conclusion of these calculations is similar; substitution of Mo by Co or Ni leads to the appearance of CUS sites that are stable under hydrotreating conditions.

Now that many aspects of the surface structures of Mo-based catalysts are well defined within this theoretical framework, it becomes possible to carry out mechanistic studies of hydrotreating reactions. At this time, the reaction pathways for the HDS of thiophene[15] and 4-methylbenzothiophene[18,21] on MoS_2 surfaces have been computed. In these studies, however, the formation and the nature of active hydrogen species (e.g., hydrides and sulfhydril groups) were not computed as a part of the reaction scheme but were assumed de facto as little is known about the actual nature of these species.

Using silver salts, Maternová[22] has been able to demonstrate and to titrate sulfhydril groups (−SH) on Mo and CoMo sulfided catalysts, nonsupported or supported on Al_2O_3. Miciuckiewicz et al. and Stuchlý et al. have further used this method on similar systems.[23] Some of these studies gave evidences of correlations of the catalytic activity and the amount of titrated −SH species. They showed that these sulfhydrils could either play an important role in hydrotreating reactions or be a measure for the sulfide phase dispersion.

Spectroscopic evidence for the presence of these −SH groups, however, is still scarce. Direct observations were obtained by inelastic neutron scattering by Wright et al.[24] and more recently by Sundberg et al.[25] on bulk and alumina-supported MoS_2 catalysts. A spectral peak at ca. 600 cm^{-1} has been assigned to a MoSH deformation mode. Other spectroscopic studies have only reported indirect evidence for the presence of −SH groups. Thus, analyzing FTIR spectra of $(Co)Mo/Al_2O_3$ catalysts, Topsøe et al. have ascribed the perturbation of the support hydroxyl groups to hydrogen bonding with acidic −SH groups.[26] They could further confirm this acidity using FTIR spectroscopy of pyridine adsorbed at high temperature.[27] More recently, Maugé et al. demonstrated an increase in Brønsted acidity related to the sulfided phase on similar catalytic systems[28,29] and could further find evidence that H_2S adsorption leads to an important increase in the Brønsted acidity of the sulfide phase.[28,30] Finally, the presence of −SH groups on Mo-based catalysts is now well recognized. This is not the case, however, for hydride species. Still, no experimental evidence for such species has been provided on MoS_2 catalysts, although such species have been found on other sulfide phases such as RuS_2.[31]

Another approach to get more insight into hydrogen activation over sulfided catalysts is the study of H_2-D_2 exchanges. Thomas et al. have studied this reaction in the case of unsupported and alumina-supported catalyst,[32−35] whereas Hensen et al. have investigated the case of sulfides supported on carbon.[36] Both

(6) Clausen, B. S.; Lengeler, B.; Candia, R.; Als-Nielsen, J.; Topsøe, H. *Bull. Soc. Chim. Belg.* **1981**, *90*, 1249.
(7) Sorensen, O.; Clausen, B. S.; Candia, F.; Topsøe, H. *Appl. Catal.* **1985**, *13*, 363.
(8) (a) Topsøe, N. Y.; Topsøe, H. *J. Catal.* **1983**, *84*, 386. (b) Bachelier, J.; Tilliette, M. J.; Cornac, M.; Duchet, J. C.; Lavalley, J. C.; Cornet, D. *Bull. Soc. Chim. Belg.* **1984**, *93*, 743.
(9) Vissers, J. P. R.; de Beer, V. J. H.; Prins, R. *J. Chem. Soc., Faraday Trans. 1* **1987**, *83*, 2145.
(10) Hensen, E. J. M.; Lardinois, G. M. H. J.; de Beer, V. H. J.; van Veen, J. A. R.; van Santen, R. A. *J. Catal.* **1999**, *187*, 95.
(11) (a) Helveg, S.; Lauritsen, J. V.; Lægsgaard, E.; Stensgaard, I.; Nørskov, J. K.; Clausen, B. S.; Topsøe, H.; Besenbacher, F. *Phys. Rev. Lett.* **2000**, *84*, 951. (b) Lauritsen, J. V.; Helveg, S.; Lægsgaard, E.; Stensgaard, I.; Clausen, B. S.; Topsøe, H.; Besenbacher, F. *J. Catal.* **2001**, *197*, 1.
(12) Byskov, L. S.; Hammer, B.; Nørskov, J. K.; Clausen, B. S.; Topsøe, H. *Catal. Lett.* **1997**, *47*, 177.
(13) Byskov, L. S.; Hammer, B.; Nørskov, J. K.; Clausen, B. S.; Topsøe, H. *J. Catal.* **1999**, *187*, 109.
(14) Byskov, L. S.; Bollinger, M.; Nørskov, J. K.; Clausen, B. S.; Topsøe, H. *J. Mol. Catal.* **2000**, *163*, 117.
(15) (a) Raybaud, P.; Hafner, J.; Kresse, G.; Toulhoat, H. *Surf. Sci.* **1998**, *407*, 237. (b) Raybaud, P.; Hafner, J.; Kresse, G.; Toulhoat, H. *Phys. Rev. Lett.* **1998**, *80*, 1481. (c) Raybaud, P.; Hafner, J.; Kresse, G.; Toulhoat, H. *Stud. Surf. Sci. Catal.* **1999**, *127*, 309.
(16) Raybaud, P.; Hafner, J.; Kresse, G.; Toulhoat, H. *J. Catal.* **2000**, *189*, 129.
(17) Raybaud, P.; Hafner, J.; Kresse, G.; Toulhoat, H. *J. Catal.* **2000**, *190*, 128.
(18) Cristol, S.; Paul, J. F.; Payen, E.; Bougeard, D.; Hafner, J.; Hutschka, F. *Stud. Surf. Sci. Catal.* **1999**, *127*, 327.
(19) Cristol, S.; Paul, J. F.; Payen, E.; Bougeard, D.; Clémendot, S.; Hutschka, F. *J. Phys. Chem.* **2000**, *104*, 11220.
(20) Travert, A.; Dujardin, C.; Maugé, F.; Cristol, S.; Paul, J. F.; Payen, E.; Bougeard, D. *Catal. Today* **2001**, *70*, 255.
(21) Cristol, S. Ph.D. Thesis, Université de Provence, France, 2000.
(22) Maternová, J. *Appl. Catal.* **1982**, *3*, 3; *Appl. Catal.* **1983**, *6*, 61.
(23) (a) Miciukewicz, J.; Zmierczak, W.; Massoth, F. E. *J. Catal.* **1987**, *96*, 915. (b) Stuchlý, V.; Zahradnikova, H.; Baranek, L. *Appl. Catal.* **1987**, *35*, 23. (c) Stuchlý, V.; Baranek, L. *Appl. Catal.* **1987**, *35*, 35.
(24) Wright, C. J.; Sampson, C.; Fraser, D.; Moyes, R. B.; Wells, P. B.; Riekel, C. *J. Chem. Soc., Faraday Trans. 1* **1980**, *76*, 1585.
(25) Sundberg, P.; Moyes, R. B.; Tomkinson, J. *Bull. Soc. Chim. Belg.* **1991**, *100*, 967.
(26) Topsøe, N. Y.; Topsøe, H.; Massoth, F. E. *J. Catal.* **1989**, *119*, 252.
(27) Topsøe, N. Y.; Topsøe, H. *J. Catal.* **1993**, *139*, 641.
(28) Petit, C.; Maugé, F.; Lavalley, J. C. *Stud. Surf. Sci. Catal.* **1997**, *106*, 157.
(29) Berhault, G.; Lacroix, M.; Breysse, M.; Maugé, F.; Lavalley, J. C.; Nie, H.; Lianglong, Q. *J. Catal.* **1998**, *178*, 555.
(30) Travert, A.; Maugé, F. *Stud. Surf. Sci. Catal.* **1999**, *127*, 269.
(31) Lacroix, M.; Yuan, S.; Breysse, M.; Dormieux-Morin, C.; Fraissard, J. *J. Catal.* **1992**, *138*, 409.

studies have led to similar conclusions. First, on these systems, the HD exchange reaction readily occurs at relatively low temperatures (353−423 K) through the sulfide phase. Moreover, there are strong indications that H_2 dissociation is heterolytic since an initial exchange occurs between $H_2(D_2)$ and $D_2S(H_2S)$. The mobility of hydrogen species is important, since in all cases an exchange of the hydrogen with the support has been observed, though different explanations for this mobility have been proposed by these groups. Finally, both groups have also studied the influence of the promotor on the rate of the exchange reaction. It has been shown by Thomas et al. that NiMo catalysts do not present a significant difference in activity as compared to a nonpromoted catalyst,[33] whereas a strong accelerating effect of the Co has been observed.[35] Similar results were obtained on (Co)Mo/C by Hensen et al. who could also show an important difference in the reaction order in H_2 and D_2 for Mo and CoMo catalysts that they have ascribed to a change in the rate-limiting step of the H_2-D_2 exchange reaction on these catalysts.[36]

As for theoretical investigations of hydrogen activation by metal sulfides, they show that hydrogen can dissociate heterolytically on MoS_2,[37] NiS_x particles,[38] and RuS_2,[39] leading to the formation of a metal hydride and a sulfhydril group. More recently, Cristol et al. have reinvestigated H_2 adsorption on MoS_2 surfaces by periodical DFT studies and could show that hydrogen species are metastable on these surfaces, the least unstable configuration being the heterolytic dissociation of hydrogen on a metal−sulfur pair.[19]

Hydrogen adsorption on Co−Mo−S surfaces has been studied by Byskov et al. who have shown that atomic hydrogen adsorption is more stable on sulfur than on Mo or on Co atoms. Accordingly, this group has exclusively studied the homolytic dissociation of hydrogen on sulfur dimers, which is exothermic and for which activation energies have been computed.[14] More recent studies, however, have shown that such dimers are not stable in hydrotreatment conditions.[16,17,19] In view of the importance of heterolytic dissociation demonstrated by most of the recent experimental studies,[32−36] it seems particularly important to reconsider hydrogen adsorption on the stable surfaces.

The aim of the present study is to investigate, using periodical DFT calculations, hydrogen activation on the $(10\bar{1}0)$ surfaces of nonpromoted and promoted MoS_2 crystallites. In the following, we first describe the theoretical methods and the models we have used throughout the present study. The energetics and structures of the model surfaces prior to H_2 adsorption are discussed and briefly compared with the results published recently in this field.[12−21] To get more insight in surface properties that are relevant for heterolytic dissociation of hydrogen, we report an investigation of the acid−base properties of these surfaces. We then describe in detail the molecular adsorption of H_2, its dissociation, and the surface diffusion of atomic species. These theoretical results are finally compared with experimental studies of the H_2-D_2 exchange reactions.

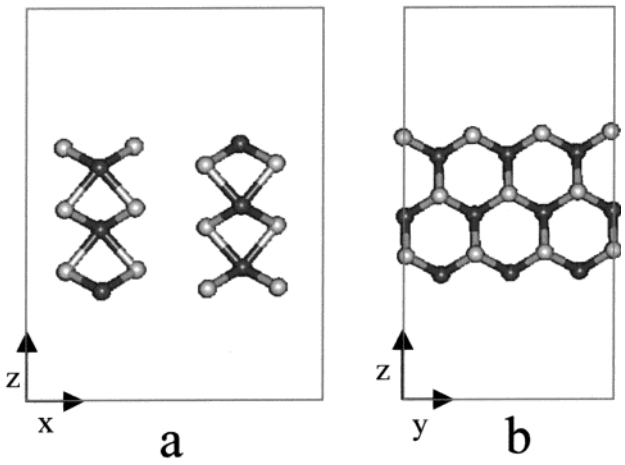

Figure 1. Representation of the supercell used for calculations, showing the axes. Dark circles, Mo atoms; light circles, S atoms.

2. Theoretical Methods

For our calculations, we have used the Vienna ab initio simulation program (VASP)[44] based on the density functional theory.[40] Exchange-correlation was treated using the functional of Perdew and Zunger[41] and corrected for nonlocal effects using the generalized gradient approximation (GGA) of Perdew et al.[42] The wave functions were expanded in plane waves, and the ionic cores were modeled by ultrasoft pseudopotentials (US-PP).[43] The solution of the Kohn−Sham equations was improved self-consistently until a difference lower than 10^{-4} eV was obtained between successive iterations. All of the ions were fully relaxed using a conjugate-gradient algorithm until all exact Hellmann−Feynman forces acting on ions are smaller than 2×10^{-2} eV $Å^{-1}$. For more details about the code, we refer the reader to other studies.[44]

The supercell used in the present study is shown in Figure 1. It contains two MoS_2 layers along the *x* direction (stacking), three Mo rows along the *y* direction, and three rows along the *z* direction. In this axis system, the (100) MoS_2 active surface is represented by the upper layers parallel to the *xy* plane, and it exhibits alternative rows of exposed molybdenum atoms and sulfur atoms which are commonly called molybdenum edges (or Mo edges) and sulfur edges (or S edges). Geometries were fully relaxed using the G point and a cutoff energy of 200 eV for the study of S, H_2S, and H_2 adsorption and 300 eV to describe NH_3 adsorption. The validity of the relative energies was further checked by single point calculations at this geometry using two k-points in the *y* direction. These settings ensure an accuracy of ca. 0.2 eV for the relative energies of the surfaces prior to hydrogen adsorption and better than 0.1 eV on the adsorption energies of hydrogen. For more details on the computation parameters and convergence checks, we refer the reader to the Supporting Information.

For the construction of promoted surfaces, we have followed the work of Raybaud et al. who have extensively studied the energetics and structures of promoted catalysts, showing that the most favorable location of Co is for the substitution of exposed Mo atoms of the metal

(32) Thomas, C.; Vivier, L.; Lemberton, J. L.; Kasztelan, S.; Pérot, G. *J. Catal.* **1997**, *167*, 1.
(33) Thomas, C.; Vivier, L.; Lescanne, M.; Kasztelan, S.; Pérot, G. *Catal. Lett.* **1999**, *58*, 33.
(34) Thomas, C.; Vivier, L.; Travert, A.; Maugé, F.; Kasztelan, S.; Pérot, G. *J. Catal.* **1998**, *179*, 495.
(35) Scaffidi, A.; Vivier, L.; Travert, A.; Maugé, F.; Kasztelan, S.; Scott, C.; Pérot, G. *Stud. Surf. Sci. Catal.* **2002**, *138*, 31.
(36) Hensen, E. J. M.; Brans, H. J. A.; Lardinois, G. M. H. J.; de Beer, V. H. J.; van Veen, J. A. R.; van Santen, R. A. *J. Catal.* **2000**, *98*, 192.
(37) Anderson, A. B.; Al-Saigh, Z. Y.; Hall, W. K. *J. Phys. Chem.* **1988**, *92*, 803.
(38) Neurock, M.; van Santen, R. A. *J. Am. Chem. Soc.* **1994**, *116*, 4427.
(39) Frechard, F.; Sautet, P. *Surf. Sci.* **1997**, *389*, 131.
(40) (a) Hohenberg, P.; Kohn, W. *Phys. Rev. B* **1964**, *136*, 864. (b) Kohn, W.; Sham, L. J. *Phys. Rev. A* **1965**, *140*, 1133.
(41) Perdew, J. P.; Zunger, A. *Phys. Rev. B* **1981**, *23*, 5048.
(42) Perdew, J. P.; Chevary, J. A.; Vosko, S. H.; Jackson, K. A.; Pederson, M. R.; Singh, D. J.; Frolais, C. *Phys. Rev. B* **1992**, *46*, 6671.
(43) Vanderbilt, D. *Phys. Rev. B* **1980**, *41*, 7892.
(44) (a) Kresse, G.; Hafner, J. *Phys. Rev. B* **1993**, *47*, 558; *Phys. Rev. B* **1994**, *49*, 14221. (b) Kresse, G.; Furthmüller, J. *Phys. Rev. B* **1996**, *6*, 15; *Phys. Rev. B* **1996**, *54*, 11169. (c) http://cms.mpi.univie.ac.at/vasp/.

edge of MoS_2 (100) surface.[17] Accordingly, we have built our surfaces by substituting from one to three molybdenum atoms of this edge, leading to metal edges presenting 0, 33, 66, and 100% Co and 33% Ni. As for the sulfur edge, we have used the most stable one under hydrotreating conditions which present a sulfur coverage of 50% (one sulfur atom per exposed molybdenum atom).[16,19]

To determine the sulfur coverages and the structure of the metallic edges, we have followed the same approach as Cristol et al.[19] by considering the thermodynamic equilibrium of these surfaces with H_2S and H_2 in the gas phase. The relative energies of the surfaces as a function of the S coverage are obtained from the energetics of the following reaction:

$$\text{surface-S}_0 + n\ \text{H}_2\text{S} = \text{surface-S}_n + n\ \text{H}_2 \qquad (1)$$

where surface-S_0 stands for the naked metallic edge (no S atom), and surface-S_n stands for the sulfided metallic edge (n sulfur atoms). The Gibbs energy of this reaction allows one to determine the stable surfaces in various experimental conditions:

$$\Delta_r G = \mu(\text{surface-S}_n) - \mu(\text{surface-S}_0) - n(\mu(\text{H}_2\text{S}) - \mu(\text{H}_2))$$

which is approximated by

$$\Delta_r G = \Delta E^\circ - n\Delta\mu$$

ΔE° is the difference between the electronic energies of the considered surfaces that are provided by VASP. $\Delta\mu$ is the difference between hydrogen sulfide and dihydrogen chemical potentials:

$$\Delta\mu(T, P_{\text{H}_2\text{S}}, P_{\text{H}_2}) = \Delta\mu^\circ(T) + RT \ln \frac{P_{\text{H}_2\text{S}}}{P_{\text{H}_2}}$$

$\Delta\mu^\circ(T)$ has been evaluated using the computed electronic energies and rotational momenta (rigid body approximation) and the experimental vibration frequencies. In typical conditions of hydrotreatment (673 K and $P_{H_2S}/P_{H_2} = 0.01$), $\Delta\mu = -5.04$ eV molecule^{-1}. In sulfiding conditions (673 K, $P_{H_2S}/P_{H_2} = 0.10$), $\Delta\mu = -4.90$ eV molecule^{-1}.

It should be noted that the thermodynamical approach we used does not take into account the total pressure, but only the $P(H_2S)/P(H_2)$ ratio. A more advanced approach,[45] taking into account the total pressure, has shown that surface structures under large excess of hydrogen − conditions which correspond to the present surfaces − are poorly affected by the total pressure.

Finally, the (100) surfaces that are relevant under given experimental conditions are obtained by computing their Boltzmann population:

$$x_i = \frac{\exp(-\Delta_r G_i/RT)}{\sum_j \exp(-\Delta_r G_j/RT)}$$

Following this, the acidic properties of the surfaces and the interactions of hydrogen with various adsorption sites have been considered, molecular adsorption as well as homolytic and heterolytic dissociation. Typical reaction pathways for hydrogen dissociation and diffusion on the surface were computed using the nudged elastic band method.[46] We successively present and discuss these results in the following sections.

3. Thermodynamically Stable Surfaces before H_2 Adsorption

In the present study, we have investigated the various surface configurations by progressively increasing the sulfur coverage of each of the three promoted surfaces and stopping once the evolution of the energies of these surfaces as a function of the sulfur coverage clearly showed that higher sulfur coverages would not lead to more stable surfaces. The energetics and the structures of the most stable surfaces are reported in Table 1 and Figure 2, respectively. Whenever it was possible, we have compared these results with the data recently published by Raybaud et al.,[16,17] and we generally found a good agreement.

Table 1. Energetics of (10$\bar{1}$0) Sulfide Surfaces[a]

Pr/(Pr + Mo)	nS	structure	ΔE/eV cell^{-1}	$\Delta_r G$/eV cell^{-1}	x_i
	0		0.00	0.00	1.73×10^{-32}
	1		−2.51	−1.93	4.37×10^{-18}
	2	**2b**	−4.73	−3.57	8.17×10^{-6}
0.00	3	**2a**	−5.99	−4.25	$1.00 \times 10^{+0}$
	4		−5.53	−3.21	1.80×10^{-8}
	0		0.00	0.00	9.39×10^{-20}
	1	**2e**	−3.12	−2.54	9.10×10^{-1}
	2	**2d**	−3.56	−2.40	8.44×10^{-2}
Co 0.33	2	**2f**	−3.39	−2.23	4.95×10^{-3}
	3	**2c**	−3.82	−2.08	3.66×10^{-4}
	3		−3.60	−1.87	9.02×10^{-6}
	4		−3.48	−1.17	5.05×10^{-11}
	0		0.00	0.00	1.11×10^{-5}
	1	**2g**	−1.24	−0.66	$0.99 \times 10^{+0}$
Co 0.66	1		0.55	1.12	4.18×10^{-14}
	2	**2h**	−1.31	−0.15	1.43×10^{-4}
	3		−1.41	0.33	3.78×10^{-8}
	0	**2i**	0.00	0.00	0.99×10^{-1}
Co 1.00	1	**2j**	−0.07	0.51	1.60×10^{-4}
	2		−0.22	0.94	9.60×10^{-8}
	0		0.00	0.00	7.79×10^{-20}
Ni 0.33	1		−3.16	−2.55	$0.99 \times 10^{+0}$
	2		−3.27	−2.23	3.96×10^{-3}

[a] Pr/(Mo + Pr), atomic fraction of promotor atom on the metallic edge; nS, number of sulfur atoms adsorbed on the metallic edge; structure, refers to Figure 2; ΔE, electronic energy difference for reaction 1 per unit cell; $\Delta_r G$, Gibbs energy difference for reaction 1 per unit cell 673 K, $H_2S/H_2 = 0.1$; x_i, Boltzman population.

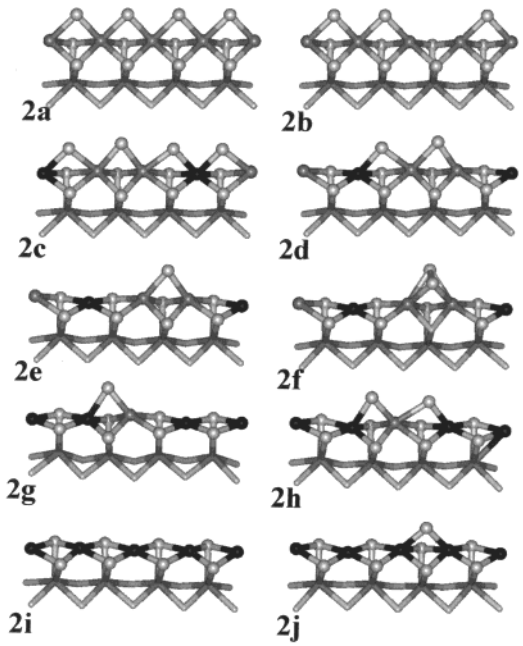

Figure 2. Representation of the stable (10$\bar{1}$0) surfaces under sulfiding conditions (673 K, $H_2S/H_2 = 0.1$). Dark gray circles, Mo; light gray circles, S; black circles, Co.

(45) Cristol, S.; Paul, J. F.; Payen, E.; Bougoard, D.; Clemendot, S.; Hutschka, F. *J. Phys. Chem. B*, in press.
(46) (a) Mills, G.; Jónsson, H. *Phys. Rev. Lett.* **1994**, *72*, 1124. (b) Mills, G.; Jónsson, H.; Schenter, G. K. *Surf. Sci.* **1995**, *324*, 305. (c) Henkelman, G.; Jónsson, H. *J. Chem. Phys.* **2000**, *113*, 9978.

For a detailed structural and electronic structure analysis of these surfaces, we refer the reader to these studies.[16,17]

The Gibbs energy variations and Boltzmann populations have been computed for "sulfiding conditions", at 673 K with a H_2S/H_2 ratio of 0.1. The surfaces presenting computed populations in the range $10^{-1}-10^{-4}$ are represented in Figure 2.

Before going into more details, we stress here that because of (i) the uncertainty of the relative energies ΔE of the surfaces, (ii) the influence of temperature and H_2S/H_2 ratio variations on chemical potential of the gas phase, and (iii) the absence of experimental data on the actual Co contents of the metal edges of promoted catalysts, care should be taken with the surface populations that are reported in this table, since in particular these values are very sensitive to slight variations of the Gibbs energies. Therefore, these values are reported to give an indication of the relative stabilities of the surface sites that such surfaces may exhibit. Accordingly, we consider that the structures presenting a computed Boltzmann population on the order of $10^{-1}-10^{-2}$ are likely to be present in large amounts, since these values are usually poorly affected by slight variations in the energies. Similarly, the structures presenting the lowest Boltzmann populations ($x_i < 10^{-5}$) are unlikely to be stable under hydrotreating conditions, although some of them might be considered as "transient" surface species that can appear locally during the reaction, especially when x_i is on the order of $10^{-5}-10^{-6}$. Last, structures presenting an intermediate Boltzmann population ($10^{-3}-10^{-4}$) are sensitive to slight variations in the energies, so that their "actual" population can reach a few percents according to the chemical potential of the gas phase or the details of calculation settings. Therefore, such structures could be relevant for catalysis, since "unstable" sites are presumably more reactive.

Unpromoted MoS_2 Molybdenum Edge. The sulfur coverage of unpromoted MoS_2 (100) surfaces has been extensively studied by Raybaud et al.[16,17] and Cristol et al.[19] Both studies show that under the working conditions of these catalysts, the most stable metallic edge presents only bridging sulfur atoms with six-fold coordinated molybdenum atoms, as shown in Figure 2a. For further comparison, we have reported in Table 1 the energetics of four unpromoted surfaces studied by Cristol et al.[19] The cost in electronic energy to remove one sulfur atom from this surface is 1.26 eV and leads to the creation of two Mo CUS sites (five-fold coordinated Mo atoms, Figure 2b). When the chemical potential of the gas phase is taken into account, the energy cost is lowered to 0.68 eV. To remove one sulfur atom is still thermodynamically unfavorable, even in the case of very low H_2S/H_2 ratios. As a result, the population of such sites is particularly low, ca. 10^{-5}.

These observations have lead Cristol et al. to conclude that these CUS sites, which are required for hydrotreating reactions, can only appear transitorily in the course of the reaction.[19,21] It should be noted that although such a conclusion was a priori unexpected, these theoretical results are in good agreement with experimental data derived from EXAFS, TPR, and IR spectroscopy studies.[19,20]

Co−Mo−S Surfaces. For a substitution of 33% of Mo by Co, the most stable surface − before thermodynamics corrections − presents a sulfur coverage of 50% (Figure 2c). This is similar to the unpromoted surface. In that case, however, the energy required to remove one sulfur atom is much lower (0.3 eV instead of 1.2 eV). Consequently, when the effect of the temperature and of the H_2S/H_2 gas phase is taken into account, the most stable surfaces present sulfur vacancies, and the 50% covered surface is not the most stable anymore ($x_i = 3.6 \times 10^{-4}$). The surface most stable in hydrotreating conditions ($x_i = 0.91$) is the 17%-covered one with a sulfur atom bridging two Mo atoms (Figure 2e). Two other surfaces presenting a S coverage of 33% are also present in these conditions. The first one ($x_i = 8.44 \times 10^{-2}$, Figure 2d) presents two two-fold coordinated sulfur atoms bridging two Mo atoms, on one hand, and a Mo and a Co atom, on the other hand. The second one ($x_i = 4.95 \times 10^{-3}$, Figure 2f) presents two two-fold coordinated sulfur atoms forming a S−S bridge.

Similar trends are observed for higher Co−Mo substitution ratios. For 66% substitution, the most stable surface before thermodynamics corrections is also 50%-covered by sulfur, and the energy required to remove one S atom is 0.1 eV, 3 times lower than in the previous case (33% Co). As result, when the gas phase is taken into account, this surface is not thermodynamically stable ($x_i = 3.78 \times 10^{-8}$), and the predominant surface presents a sulfur coverage of 17%, with a sulfur atom bridging one Co and one Mo atom ($x_i = 0.99$, Figure 2g). A second surface, presenting a sulfur coverage of 33%, is much less stable ($x_i = 1.43 \times 10^{-4}$, Figure 2h) but might appear in nonnegligible amount, for example, in sulfur-rich conditions. Finally, when the metallic edge is fully substituted by cobalt, two surfaces may appear. The most stable surface is not covered at all by sulfur and presents only four-fold coordinated Co atoms ($x_i = 0.99$, Figure 2i), whereas a second structure with sulfur atoms bridging two cobalt atoms is likely to appear in sulfur-rich conditions ($x_i = 1.60 \times 10^{-4}$, Figure 2j).

Ni−Mo−S Surfaces. To compare the effect of Ni and Co, we have investigated Ni-promoted surfaces for a surface substitution ratio of 33% Ni. The structure of these surfaces is similar to the Co case (Figure 2c−f). As for the energetics (Table 1), the most stable surface is also 17%-covered by sulfur, but it is significantly more abundant ($x_i > 0.99$) than the corresponding CoMo surface (Figure 2c, $x_i = 0.91$). The relative energy of this surface with respect to the naked surface is the same as in the unpromoted and the Co cases (−2.5 eV). On the other hand, the surface presenting a sulfur atom bridging one Mo and one Ni atom has a lower stability than the analogous Co−Mo−S surface depicted in Figure 2d, which may be ascribed to the lower stability of Ni−S bonds as compared to Co−S bonds. Therefore, the influence of Ni on the surface structure is essentially similar to the Co case, the formation of Ni−S bonds being even less favorable than Co−S bonds.

Influence of the Promotor on Surface Structure. Finally, the striking difference with the unpromoted case is that Mo substitution by Co or Ni leads to the creation of CUS sites and sulfur dimers that are stable under the working conditions of these catalysts. This result is in good agreement with the previous studies of Byskov et al.[13] and Raybaud et al.[17] who have provided detailed explanations on the electronic origin of this effect of the promotor atom on the surface structure. From an elementary chemical point of view, one can consider a $[MoS]^{2+}$ unit on the stable MoS_2 surface to be replaced by a Co^{2+} or Ni^{2+}, hence maintaining charge neutrality. From a structural point of view, the promoted surfaces may be considered as resulting from a balance between the sulfur

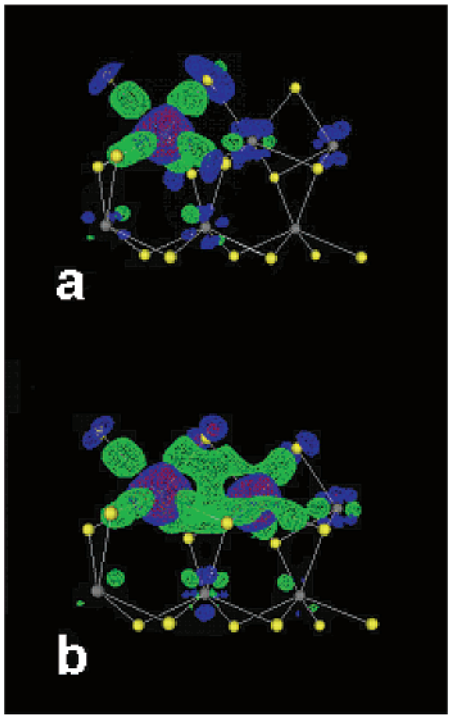

Figure 3. Electron density difference maps showing the effect of Mo substitution by Co on the (10$\bar{1}$0) surface. Green zones, electron density depletion; red and blue zones, electron density accumulation. (a) One Mo atom substituted, (b) two Mo atoms substituted.

coordination of the exposed molybdenum atoms that tend to be six-fold coordinated and the sulfur coordination of cobalt or nickel atoms that tend to be four-fold coordinated when the sulfur potential of the gas phase is taken into account.

In Figure 3 are reported electron density difference maps that clearly illustrate the effect of the substitution of one (Figure 3a) and two (Figure 3b) Mo atoms by cobalt atoms on the most stable MoS_2 surface (Figure 2a). Schematically, substitution of one Mo by Co (Figure 3a) leads to a withdrawing of electrons from the metal−sulfur bonding states (green zones) and an increase of electron density in the metal−sulfur antibonding orbitals shown by the important electron density around the Co atom and the ring around the bridging sulfur atoms (blue zones). Besides, a small increase in electron density is also observed around the neighboring Mo atoms (d states), that could be induced by the sulfur atoms of the Mo-coordination sphere that bridge the cobalt atom. Harris and Chianelli have already reported such an increase for cluster calculations.[42] Similar but amplified effects are observed for a higher substitution ratio (Figure 3b). The electron withdrawal from Co−S−Co bonding states, on one hand, and the increase in electron density around the sulfur atom bridging two Co atoms, on the other hand, are more important than in the case of the sulfur atoms bridging one Co and one Mo atom. Finally, these electronic modifications are rather local since they only occur in the first (sulfur atoms) and second (metal atoms) coordination sphere of the Co atoms.

Influence of the Promotor on Surface Acidity. To probe the acidic properties of the stable surfaces presented in Figure 2, we have monitored their interaction with ammonia. In Table 2 are reported adsorption energies and selected structural data for NH_3 coordination on Mo, Co, and Ni cations presenting different sulfur coordinations.

Table 2. NH_3 Adsorption on Lewis Acid Sites of (10$\bar{1}$0) Surfaces[a]

cation	rM–N/Å	ΔE/eV
Mo_{VI}	2.35	−0.45
Mo_{V}	2.36	−0.99
Co_{V}	2.16	−0.17
Co_{IV}	2.09	−1.17
Ni_{V}	2.27	−0.39

[a] rM−N, metal−nitrogen distance; ΔE, difference in electronic energies, $\Delta E = E(\text{surface-NH}_3) - E(\text{surface}) - E(\text{NH}_3)$.

Whatever the nature of the metal ion and its coordination environment, NH_3 adsorption is always exothermic, hence demonstrating the acidic character of these surface sites. The strength of the acid−base interaction is strongly dependent on the nature of the cation, since for an identical sulfur coordination the adsorption energies decrease according to the ranking Mo > Co > Ni.

For a given coordination, this ranking is the same as the one of metal−sulfur bond strengths. On the other hand, the second factor governing the Lewis acid strength of these cations is their sulfur coordination which, as it increases, tends to decrease their Lewis acidity, as could be expected from straightforward application of the bond order conservation principle.[47]

Finally, in view of the data reported in Table 2, on one hand, and the surface structures that we have derived from thermodynamical calculations (Figure 2), on the other hand, it clearly appears that Co and Ni promotors also enhance the surface Lewis acidity by inducing the creation of stable Mo CUS sites which are among the strongest ones on these surfaces.

This effect of Co on the Lewis acidity of the surface is in excellent agreement with the work of Berhault et al. who have shown by FTIR spectroscopy that after sulfidation, $CoMo/SiO_2$ catalysts present stronger Lewis acid sites as compared to a Mo/SiO_2 catalyst.[29]

4. Hydrogen Adsorption

The stable sulfide surfaces represented on Figure 2 present many potential adsorption sites for dissociation of hydrogen, either homolytic on sulfur dimers or heterolytic on metal−sulfur pairs. We have investigated several configurations for typical cases, on the basis of the local environment of the dissociation site. In the following, the heterolytic dissociation sites are denoted according to the coordination number of the molybdenum atom, the coordination of the sulfur atom, and the atoms to which it is bound, for example, $Mo_X-S_{II}(Mo_X,Mo_Y)$. The structures and the energetics of the resulting surfaces are reported in Figures 4−8 and Table 3, respectively.

Unpromoted Surfaces. As previously shown by Cristol et al.,[19] hydrogen dissociation on the Mo edge of the most stable surface (Figure 2a) is always endothermic whatever the final geometry considered. The less unfavorable reaction (ΔE = +0.27 eV) corresponds to hydrogen dissociation on a six-fold coordinated Mo and a sulfur bridging two six-fold coordinated molybdenum atoms, that is denoted by $Mo_{VI}-S_{II}(Mo_{VI},Mo_{VI})$. The resulting surface presents a Mo−H and a S−H group (Figure 4a). The endothermicity of hydrogen dissociation on this surface may be explained considering that the molybdenum edge of the surface does not present any unsaturated Mo atom.

(47) (a) Shustorovich, E. *Surf. Sci. Rep.* **1986**, *6*, 1. (b) Shustorovich, E. *Adv. Catal.* **1990**, *37*, 101.

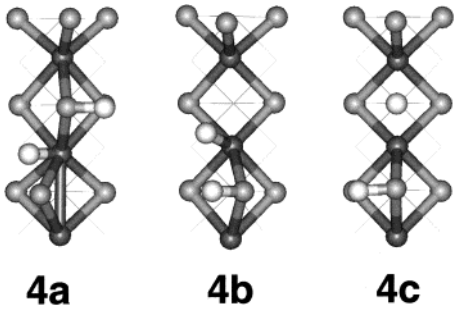

Figure 4. Representation of unpromoted ($10\bar{1}0$) MoS_2 surfaces after heterolytic addition of hydrogen. Dark circles, Mo; light circles, S; white circles, H.

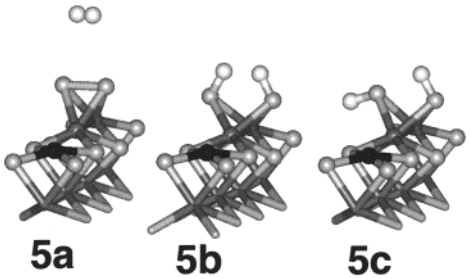

Figure 5. Representation of stable configurations of ($10\bar{1}0$) Co−Mo−S surfaces after homolytic addition of hydrogen. Dark gray circles, Mo; light gray circles, S; black circles, Co; white circles, H.

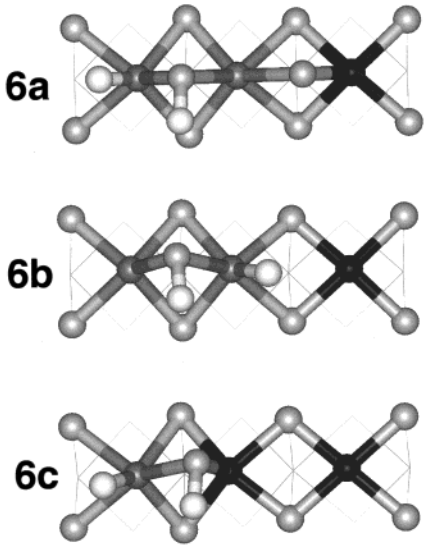

Figure 6. Representation of Co−Mo−S ($10\bar{1}0$) surfaces after heterolytic addition of hydrogen on Mo−S pairs. Dark gray circles, Mo; light gray circles, S; black circles, Co; white circles, H.

Two stable geometries were found for the addition of hydrogen to the $Mo_V-S_{II}(Mo_V,Mo_{VI})$ site of the defective surface (Figure 2b). The first one leads to the formation of one S−H and one Mo−H group and is endothermic by +0.1 eV (Figure 4b). For the second one (Figure 4c), the hydride connects two Mo atoms in a bridging position, within the Mo plane. Evidently, such a position was impossible on the previous surface because of the presence of a bridging sulfur atom. This adsorption mode is slightly exothermic (−0.10 eV). However, considering (i) the large translation entropy loss occurring during the adsorption reaction and (ii) the low population of such sites, the number of hydrogen atoms on the surface in equilibrium with the gas phase should be very small.

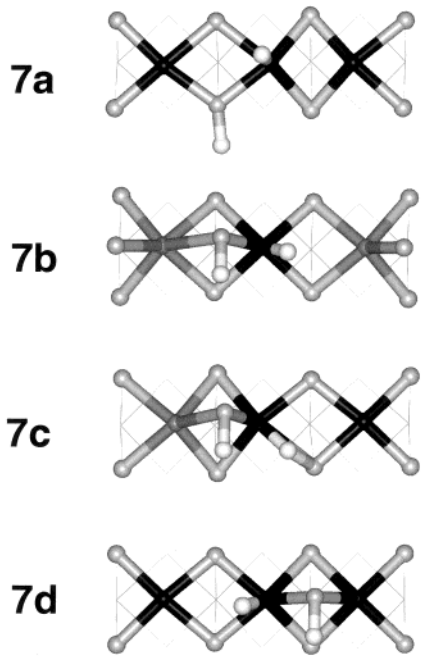

Figure 7. Representation of Co−Mo−S ($10\bar{1}0$) surfaces after heterolytic addition of hydrogen on Co−S pairs. Dark gray circles, Mo; light gray circles, S; black circles, Co; white circles, H.

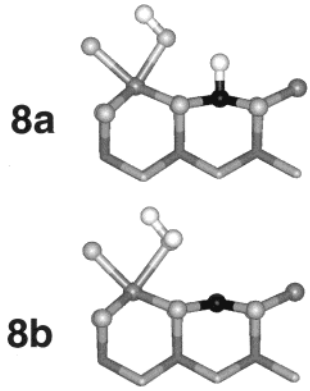

Figure 8. Representation of Ni−Mo−S ($10\bar{1}0$) surfaces after heterolytic addition of hydrogen on Ni−S pairs. Dark gray circles, Mo; light gray circles, S; black circles, Ni; white circles, H.

Any other adsorption geometry is endothermic. Thus, heterolytic dissociation on a $Mo_{VI}-S_{II}(Mo_V,Mo_{VI})$ site of the defective surface (Figure 2b) is endothermic by +0.49 eV. Interestingly, this value is slightly increased as compared to the heterolytic addition on the most stable surface (+0.27 eV), which can be understood in terms of the bond order conservation model; removing one sulfur atom from the surface induces an increase of the neighboring Mo−S bonds strength (the $Mo_{VI}-S_{II}$ distance is decreased from 2.51 to 2.43 Å), that in turn reduces the ability of these S and Mo atoms to form new bonds with hydrogen.

Promoted Surfaces. Homolytic Dissociation on Sulfur Dimers. Among the various surfaces that we have investigated, only one presents a stable sulfur dimer (Figure 2f) that may lead to homolytic dissociation, resulting in the reduction of the sulfur dimer. Three stable configurations for hydrogen interaction with this dimer are reported in Figure 5.

The molecular adsorption of hydrogen (Figure 5a) is athermic (+0.03 eV), and neither the hydrogen bond length nor the

sulfur−sulfur distance is significantly modified upon adsorption, revealing a weak interaction. On the other hand, two configurations were found stable for homolytic dissociation. The first one (Figure 5b) is also athermic (+0.01 eV), which could be ascribed to steric constraints between the two protons that are separated only by 1.77 Å. The second configuration (Figure 5c), however, is clearly exothermic (−0.19 eV). Similar results were obtained in the case of H_2 dissociation on the same kind of sulfur dimer on an unpromoted surface.[48] Byskov et al.[14] have reported activation energies on the order of 0.6 eV for such a dissociation.

Heterolytic Dissociation on Mo−S Pairs. In Figure 6 are represented three stable configurations for the heterolytic dissociation of hydrogen on molybdenum−sulfur pairs.

The first case (Figure 6a) corresponds to the heterolytic dissociation of H_2 on a five-fold coordinated Mo and a sulfur bridging two molybdenum atoms, five- and six-fold coordinated, that is denoted by $Mo_V-S_{II}(Mo_V, Mo_{VI})$. In this case, the dissociation is clearly endothermic, by +0.51 eV. It is interesting to note that it is even more endothermic than in the case of the unpromoted MoS_2 surface for hydrogen dissociation on a Mo CUS site presenting the same local environment, except for the substitution of a Mo by a Co at the neighboring dissociation site. Such a difference may be explained in the following way: replacement of Mo by Co reduces the metal−sulfur bond energy, which in turn enhances neighboring S−Mo bonds. As a consequence, the bonding of H to Mo weakens, and hence the thermodynamics of H_2 dissociation become less favorable.

The second case, $Mo_V-S_{II}(Mo_V, Mo_V)$, is very similar (Figure 6b), except that the second molybdenum atom to which the sulfur atom is bound is also five-fold coordinated instead of six-fold. The dissociation energy is still endothermic (+0.44 eV) and very close to the dissociation energy computed for the previous case.

The third case we have investigated is depicted in Figure 6c. It corresponds to H_2 heterolytic dissociation on a $Mo_V-S_{II}(Mo_V, Co_V)$ site. It strongly differs from the previous ones, in that the sulfur atom is bridging a molybdenum and a cobalt atom. In that case, the dissociation energy is significantly different and is slightly exothermic (−0.08 eV). Because the cobalt atom tends to increase the electron density around the bridging sulfur (Figure 3), we mainly ascribe this exothermicity to the ability of the bridging sulfur atom to bind the proton, that would result from this higher electron density, which is bonding for hydrogen (p-like orbitals, Figure 3).

Heterolytic Dissociation on Co−S Pairs. Four configurations for the heterolytic dissociation of hydrogen on cobalt−sulfur pairs are represented in Figure 7.

The first surface (Figure 7a) corresponds to the most stable surface for full substitution of molybdenum by cobalt. In that case, the only possibility for heterolytic dissociation is on a site formed by a four-fold coordinated Co atom and a three-fold coordinated sulfur of the basal plane. The dissociation is athermic, which is due to the low energy of the resulting S−H bond, as the sulfur atom is four-fold-coordinated. Hydrogen bonding of the proton with the second MoS_2 sheet might stabilize this species, the two closest sulfur atoms being at 2.76 and 2.97 Å from the proton.

(48) Cristol, S.; Paul, J. F.; Payen, E., to be published.

Table 3. Energetics of Heterolytic Dissociation of H_2 on $(10\bar{1}0)$ Sulfide Surfaces[a]

structure	dissociation site	ΔE/eV	E_{act}(ads)/eV	E_{act}(des)/eV
4a	$Mo_{VI}-S_{II}(Mo_{VI}, Mo_{VI})$	0.41	0.97	0.56
	$Mo_{VI}-S_{II}(Mo_V, Mo_{VI})$	0.49		
4b	$Mo_V-S_{II}(Mo_V, Mo_{VI})$	0.10	0.55	0.45
4c	$Mo_V-S_{II}(Mo_V, Mo_{VI})$	−0.10		
6a	$Mo_V-S_{II}(Mo_V, Mo_{VI})$	0.51	0.79	0.28
6b	$Mo_V-S_{II}(Mo_V, Mo_V)$	0.44		
6c	$Mo_V-S_{II}(Mo_V, Co_V)$	−0.08		
7a	$Co_{IV}-S_{III}(Co_{IV}, Co_{IV}, Mo_{VI})$	0.04		
7b	$Co_V-S_{II}(Co_V, Mo_{VI})$	−0.15	0.52	0.67
7c	$Co_V-S_{II}(Co_V, Mo_V)$	0.51		
7d	$Co_V-S_{II}(Co_V, Co_V)$	−0.55	0.34	0.91
8a	$Ni_V-S_{II}(Ni_V, Mo_V)$	0.50		

[a] ΔE, difference in electronic energies, $\Delta E = E(\text{surface-}H_2) - E(\text{surface}) - E(H_2)$; E_{act}(ads), activation energy for H_2 dissociation; E_{act}(des), activation energy for the desorption of dissociated species.

The second case, $Co_V-S_{II}(Co_V, Mo_{VI})$, corresponds to the dissociation on a cobalt atom and a sulfur atom bridging one cobalt and one molybdenum atom (Figure 7b). The dissociation is exothermic (−0.15 eV), and it differs by 0.66 eV as compared to the heterolytic dissociation on the $Mo_V-S_{II}(Mo_V, Mo_{VI})$ site on the same surface (Figure 6a). The coordination of the sulfur atom to the cobalt may explain this difference for a large part, since in the case of molybdenum−sulfur pairs, this could lower the dissociation energy by ca. 0.5 eV. The relative stabilities of hydride species (Co−H vs Mo−H) should also be considered in the energetic balance, but we will show later that their bond energy is similar (section 6).

The third case (Figure 7c) corresponds to the dissociation on a $Co_V-S_{II}(Co_V, Mo_V)$ site. The dissociation is clearly exothermic (−0.51 eV). In this case, the "hydride" species is bridging the cobalt and one sulfur atom of the basal plane. This particular configuration has to be related to an important distortion of the surface around the dissociation site that is already present before hydrogen adsorption (Figure 2f). A similar geometry for this site has also been reported by Raybaud et al.[17]

Finally, the fourth case (Figure 7d) corresponds to the dissociation on the $Co_V-S_{II}(Co_V, Co_V)$ site that is also present on the surfaces fully substituted by Co (Figure 2i). The dissociation on this site is the most exothermic with respect to all the previous cases and is −0.55 eV. The energy difference with the dissociation on the $Co_V-S_{II}(Co_V, Mo_{VI})$ is around 0.4 eV. Interestingly, this value is similar to the difference in energy for the dissociation on $Mo_V-S_{II}(Mo_V, Mo_V)$ and $Mo_V-S_{II}(Mo_V, Co_V)$ sites, respectively. As previously, we may consider that the coordination environment of the sulfur atom that is bridging to two cobalt atoms causes this large energy difference.

Finally, at this stage of the study, considering only the local environment of the dissociation site and discarding the particular case of Figure 7b, simple energy differences between various configurations show that substitution of one molybdenum atom by one cobalt leads to (i) a decrease in the stability of Mo−H species and (ii) a higher proton affinity of sulfur atoms bridging one or two Co atoms.

Heterolytic Dissociation on Ni−S Pairs. Figure 8a reports a stable configuration that has been obtained for heterolytic dissociation of hydrogen on the $Ni_V-S_{II}(Ni_V, Mo_{VI})$ site. The dissociation on this site is slightly endothermic, by ca. 0.06 eV,

Table 4. NH_3 Adsorption on −SH Groups of $(10\bar{1}0)$ Surfaces[a]

	*r*S−H/Å	*r*S−H···NH_3/Å	$\Delta r/r_0$	*r*H···N/Å	ΔE/eV
(Mo,Mo)S−H	1.363	1.55	0.137	1.48	−0.47
(Co,Mo)S−H	1.361	1.47	0.080	1.60	−0.49
(Co,Co)S−H	1.369	1.45	0.059	1.70	−0.37

[a] *r*S−H, sulfur−hydrogen bond length before NH_3 adsorption; *r*S−H···NH_3, sulfur−hydrogen bond length after NH_3 adsorption; $\Delta r/r_0$, S−H bond length extension upon adsorption; *r*H···N, hydrogen−nitrogen bond length; ΔE, difference in electronic energies, $\Delta E = E(\text{surface-NH}_3) - E(\text{surface}) - E(NH_3)$.

and leads to the cleavage of the Ni−S bond, resulting in the formation of a monodentate −SH group and a Ni_{IV} hydride species. The second stable configuration for the addition of H_2 on this site is represented in Figure 8b and corresponds to the formation of H_2S, which is an exothermic process (−0.5 eV). Evidently, this case strongly differs from the dissociation on the analogous site $Co_V-S_{II}(Co_V, Mo_{VI})$ which was exothermic and for which the Co−S bond remained stable after dissociation (Figure 5c). To a first approximation, this difference may be ascribed to the much lower stability of Ni−S bonds as compared to Co−S bonds that we have mentioned previously.

Brønsted Acidity of the Resulting Surfaces. To check quantitatively the aforementioned variation of the sulfur basicity according to its coordination environment, we have monitored the interaction of the sulfhydril groups with ammonia. Table 4 reports selected structural data and adsorption energies for the hydrogen bonding of NH_3 with three −SH groups selected according to the coordination environment of the sulfur atom.

The adsorption of ammonia on these −SH groups is clearly exothermic, on the order of 0.4−0.5 eV, indicating that such groups present a Brønsted acidic character. On an energetic basis, one can make a clear distinction between the SH group bridging two Mo atoms, on one hand, and those bridging one or two cobalt atoms, on the other hand, the latter being less acidic that the former one. On a structural point of view, it is interesting to look at the S−H bond extension that occurs upon hydrogen bonding with ammonia, since it is a usual indicator for Brønsted acidity. This bond stretching varies according to the ranking (Mo,Mo)S−H > (Mo,Co)S−H > (Co,Co)S−H.

This clearly suggests that as a ligand of surface sulfur atoms, Co decreases the Brønsted acid strength of sulfhydril groups or, otherwise stated, increases the sulfur basicity. This trend is in excellent agreement with the strong variations in H_2 dissociation energies on the various metal−sulfur pairs previously described.

5. Reaction Paths for Heterolytic Dissociation of Hydrogen

Unpromoted Surfaces. The geometry of the transition state (TS) leading to the heterolytic dissociation of H_2 on the $Mo_{VI}-S_{II}(Mo_{VI}-Mo_{VI})$ site of the unpromoted surface is reported in Figure 9a. The activation energy of the elementary reaction is 0.97 eV. As the reaction is endothermic (+0.41 eV), the barrier associated to the reverse reaction is much smaller (0.56 eV). The final geometry of the elementary step does not match exactly the geometry of the most stable adsorption mode (Figure 4a). To get this stable situation, one of the hydrogen atoms must jump from one side of the metallic edge to the other one. However, as this displacement does not include the breaking or the formation of bonds, it is reasonable to assume that this elementary step has a low activation energy.

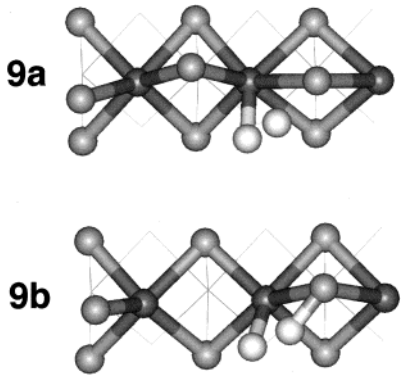

Figure 9. Representation of the transition states for the heterolytic addition of hydrogen on unpromoted MoS_2 $(10\bar{1}0)$ surfaces. Dark gray circles, Mo; light gray circles, S; white circles, H.

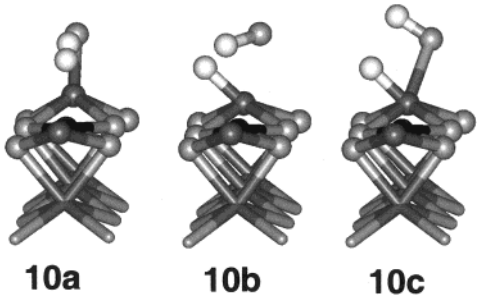

Figure 10. Representation of (a) initial state, (b) transition state, and (c) final state for the heterolytic addition of hydrogen on a Mo−S pair of the Co−Mo−S $(10\bar{1}0)$ surface. Dark gray circles, Mo; light gray circles, S; black circles, Co; white circles, H.

The TS leading to H_2 addition on the $Mo_V-S_{II}(Mo_V,Mo_{VI})$ site of the unpromoted defective surface is depicted in Figure 9b. Starting from the physisorption mode, the computed activation energy is 0.55 eV for the formation of one S−H and one Mo−H group (Figure 4b). The migration of the hydride to the more stable bridging position (Figure 4b) is very easy (E_a = 0.05 eV).

Promoted Surfaces. In Figure 10 are reported three snapshots of the minimum energy reaction path for the dissociation on $Mo_V-S_{II}(Mo_V, Mo_{VI})$, which is the most endothermic on the promoted surfaces.

The first image (Figure 10a) corresponds to the molecular adsorption of hydrogen that is almost athermic. The hydrogen bond length is 0.79 Å that has to be compared with 0.75 Å for the free molecule. The TS (Figure 10b) is located at 0.79 eV above the molecular adsorption. The important extension of the molybdenum−sulfur bonds that is a consequence of hydrogen dissociation may significantly contribute to this energy. Figure 10c represents the final state of the elementary reaction.

Figure 11 reports six snapshots and the energy diagram of the minimum energy reaction path for the dissociation on the $Co_V-S_{II}(Co_V, Co_V)$ site, which is the most endothermic case of hydrogen dissociation on these surfaces. The energy diagram for this path is plotted as function of the H−H distance. The first image (Figure 11a) clearly shows that the configuration for molecular adsorption of H_2 on this site is quite different from the previous case. First, the hydrogen bond length is much higher (0.86 vs 0.79 Å), showing that as an adsorption center, cobalt favors activation of molecular hydrogen. Second, a surface reconstruction occurs upon molecular adsorption, which leads to an important displacement of the bridging sulfur atom

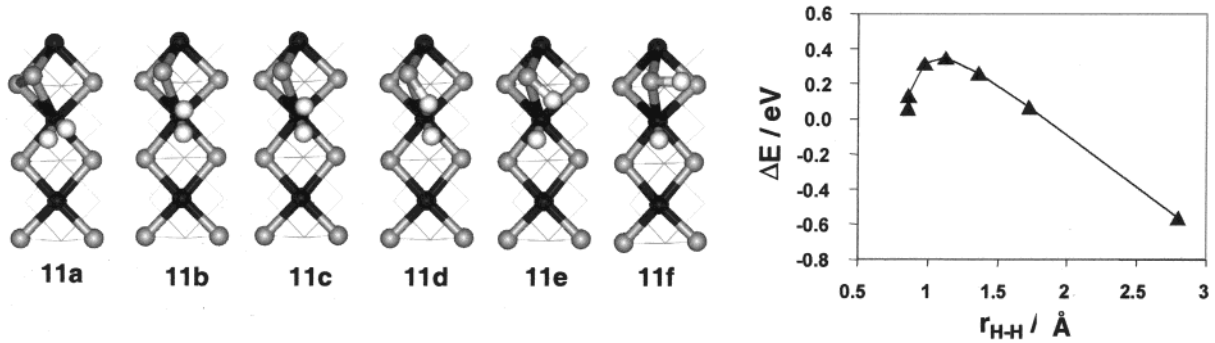

Figure 11. Snapshots of the minimum energy reaction path for the heterolytic addition of hydrogen on a Co−S pair of the Co−Mo−S ($10\bar{1}0$) surface. Dark gray circles, Mo; light gray circles, S; black circles, Co; white circles, H. Graph: Energy diagram as a function of the H−H distance.

that now forms a sulfur bridge with a sulfur atom of the basal plane. This molecular adsorption is slightly exothermic, +0.06 eV. The reaction pathway is straightforward. First, the hydrogen molecule undergoes a slight rotation, and the bridging sulfur comes back in the molybdenum plane; this leads simultaneously to an extension of the H−H distance and a reduction of the hydrogen−bridging sulfur distance. The dissociation then occurs, and the stable dissociated state is finally reached. The activation energy for this dissociation is 0.34 eV, which is much lower than in the previous cases. Such a low activation barrier may be ascribed to the effect of cobalt that (i) directly favors the activation of molecular hydrogen and (ii) increases sulfur reactivity and flexibility.

6. Surface Diffusion of Dissociated Species

Several pathways for the surface diffusion of dissociated species were computed, for displacements from metal atom to metal atom, as well as from sulfur to metal. Figures 12 and 13 report snapshots of the diffusion paths on unpromoted and Co promoted surfaces, respectively.

Unpromoted Surfaces. Once the hydrogen molecules have been dissociated on the most stable molybdenum edge (Figure 12a), the activation energies for the diffusion are relatively small. The migration of one hydrogen from one Mo_{VI} atom to an S_{II} atom is almost athermic (+0.04 eV, Figure 12a−c), showing that the energies associated to the Mo−H and to the S−H bonds are close. This is in good agreement with a previous study[19] where it was shown that the energies associated with the formation of two −SH groups, on one hand, and one −SH and one Mo−H group, on the other hand, are similar, within 0.1 eV.

The activation energy for this diffusion step is 0.54 eV, and the direct reaction is as easy as the reverse one. We have been looking for an elementary diffusion of the hydride species directly from one Mo atom to a second one. Whatever the computational technique used, however, we have not been able to determine a direct reaction, and an S−H intermediate group has always been created.

The diffusion of hydrogen on the defective surface may be decomposed into two parts. In the first part, we have investigated the diffusion of hydrogen atoms between fully coordinated atoms (i.e., Mo_{VI} and S_{II}). The activation energy of the diffusion from the S atom to the Mo one is 0.39 and 0.25 eV for the reverse reaction (Figure 12d−f). These two values match the values calculated on the most stable surface, showing that the electronic influence of the vacancy on this surface has a small spatial

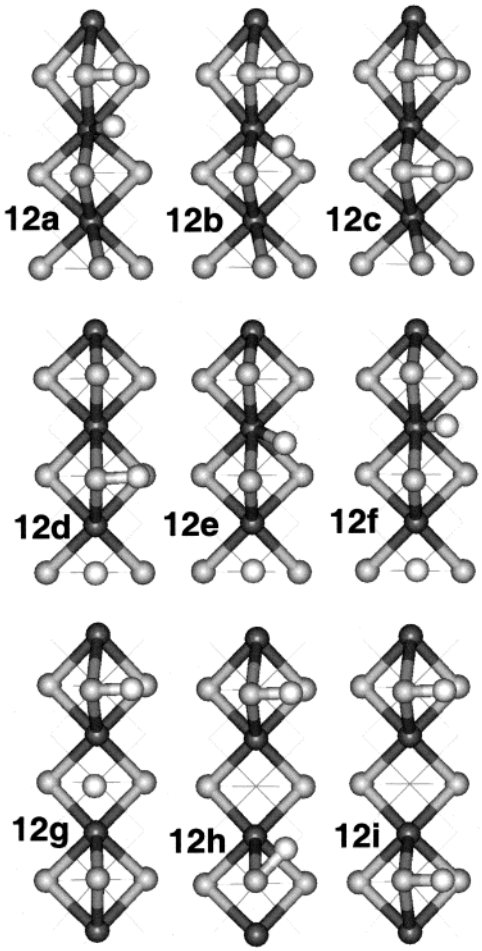

Figure 12. Representation of initial states (left), transition states (middle), and final states (right) for hydrogen diffusion on the unpromoted MoS_2 ($10\bar{1}0$) surface. Dark gray circles, Mo; light gray circles, S; white circles, H.

extension. In the second part, we have investigated the diffusion of the hydrogen originating from the bridging position between two Mo's. The activation for this displacement to the next sulfur atom is 0.93 eV (Figure 12g−i). This important activation energy is even larger than the desorption activation energy (0.72 eV). Taking into account the small number of such vacancies on these surfaces, however, such pathways should have a very small influence on the overall diffusion on MoS_2 surfaces.

Promoted Surfaces. Figure 13a corresponds to the diffusion of a hydride species from the five-fold coordinated Co atom that is involved in the heterolytic dissociation on the Co_V-S_{II}-

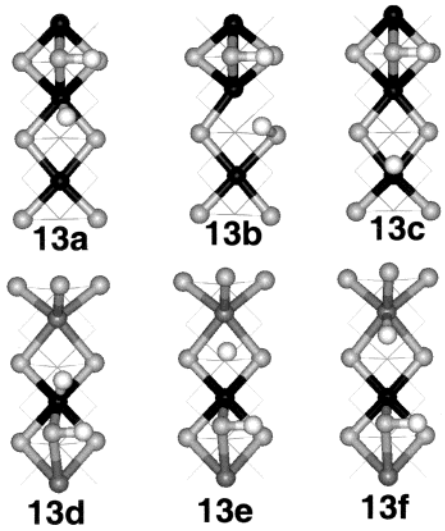

Figure 13. Representation of initial states (left), transition states (middle), and final states (right) for hydrogen diffusion on the Co−Mo−S ($10\bar{1}0$) surface. Dark gray circles, Mo; light gray circles, S; black circles, Co; white circles, H.

(Co_V, Co_V) site to the vicinal four-fold coordinated Co atom. In this case, hydrogen diffuses via the three-fold coordinated sulfur atom of the basal plane that bridges the two cobalt atoms. This process is weakly activated by 0.29 eV, and both initial and final configurations are of similar energy, showing that Co_V and Co_{IV} hydride species have a similar stability. Figure 13b depicts the reaction path for the diffusion of a hydride species from a Co_V to a Mo_V center. In this case, the hydride species does not diffuse via a three-fold coordinated bridging sulfur atom but is directly transferred from the Co_V atom to the Mo_V atom. This can be explained by the shorter distance (1.70 Å vs 2.35 Å) that the hydride has to cross from the initial to the final states of the elementary process. This hydride "hopping" has a similar activation energy as in the previous case, and, interestingly, the energy difference between the initial and the final state is on the order of 0.04 eV. From this, we deduce that Co_V−H and Mo_V−H species have a similar stability since the initial and final configurations (Figure 13d−f) only differ by the nature of the metal atom to which the hydride species is bound. This similar stability clearly shows that the nature of the hydride species that is formed after H_2 dissociation is not likely responsible for the important changes in the dissociation energy of hydrogen on Mo−S and Co−S pairs. These are on the order of 0.5 eV. Hence, the energetic balance for hydrogen heterolytic dissociation is mainly governed by the stability of the resulting −SH groups as mentioned before.

7. Implications for the H_2−D_2 Exchange Reaction and Hydrotreating Reactions

The H_2−D_2 exchange reaction consists of three elementary steps: (i) H_2 and D_2 adsorb dissociatively on the catalyst, (ii) the dissociated species diffuse over the surface so that two isotopic species can meet, and finally (iii) recombinative desorption occurs, leading to the formation of HD species in the gas phase.

In the case of the unpromoted ($10\bar{1}0$) MoS_2 stable surface, we have shown that the activation energies for the heterolytic dissociation of hydrogen are on the order of 1.0 eV. This is in all cases much higher than either the desorption (ca. 0.6 eV) or the diffusion of dissociated species (ca. 0.3−0.4 eV). Therefore, the rate-limiting step of this exchange reaction is the dissociation of dihydrogen and dideuterium on the surface. This implies that the overall rate of reaction is proportional to the amount of H_2 and D_2 present in the gas phase, or, in other words, it is first order in H_2 and D_2.

For the promoted surfaces we have shown that when the dissociation occurs on Co−S pairs, desorption of dissociated species is in most cases much more difficult (up to 0.9 eV) than either the dissociation (as low as 0.3 eV) or the diffusion (ca. 0.3 eV). Therefore, in this case, the rate-limiting step for the H−D exchange reaction is the recombinative desorption of dissociated species. This implies that the overall rate is proportional to the amount of dissociated species, that is, half order in H_2 and D_2.

This change in the rate-limiting step of the H−D exchange reaction which is predicted by our theoretical results on the nonpromoted MoS_2 and promoted Co−MoS_2 ($10\bar{1}0$) surfaces is in excellent agreement with the experimental kinetic data reported by Hensen et al. in the case of Mo/C and CoMo/C catalysts,[36] thus demonstrating the crucial role of Co−S pairs in hydrogen activation on promoted catalysts.

For NiMo sulfide catalysts, the activity data reported by Thomas et al. show that the Ni promotor does not significantly change the activity of these catalysts in the H−D exchange reaction.[33] Our theoretical calculations have shown that Ni−S pairs are not very stable on these surfaces. Even when such sites are present on these surfaces, they do not to provide an efficient way for hydrogen activation. This would lead to the cleavage of the Ni−S bond and possibly to the departure of the sulfur atom from the surface under the form of H_2S, the latter resulting in a more stable surface (Table 1). Therefore, according to our calculations, the only stable heterolytic dissociation sites of hydrogen on the ($10\bar{1}0$) Ni−Mo−S surface are Mo−S(Mo,Mo) pairs that, as shown by our calculations on Co−Mo−S surfaces, would essentially behave in a similar way as the Mo−S pairs of unpromoted MoS_2 surfaces. This hypothesis would explain, at least in part, the experimental results of Thomas et al.[33]

Finally, the present theoretical results as well as the previous experimental studies[34,36,37] clearly show that Ni and Co have a very different effect on the activation of hydrogen on Mo-based catalysts.

It is well known that NiMo and CoMo catalysts present significant differences of activity and selectivity in hydrotreating reactions. In particular, NiMo catalysts are usually more active and selective for hydrogenation reactions. From this, one may be tempted to conclude that NiMo catalysts are more efficient for hydrogen activation than are CoMo catalysts. Our calculations together with H_2/D_2 studies, however, clearly show that this is not the case. Obviously, hydrotreatment reactions are complex processes where, besides hydrogen activation, many parameters have to be taken into account: adsorption of the reacting molecule, hydride or proton attack, and competitive adsorption with products (hydrocarbons, H_2S, NH_3, ...). In view of the present results, it is clear that hydrogen activation is not the rate-limiting step for these reactions. The computed activation energies for hydrogen dissociation are low, which is in good agreement with experimental H_2/D_2 experiments that show that H_2 dissociation readily occurs at low temperatures. Actually,

to the best of our knowledge, no recent kinetic study has ever shown that hydrogen dissociation could be the rate-limiting step of these reactions.

On the other hand, our calculations show that the nature of the promotor has a strong influence on the configuration and the adsorptive properties of these surfaces. Therefore, the activation of the reacting molecule or reaction inhibition by H_2S and NH_3 might strongly differ on these surfaces and could partly explain the differences in the promotional behavior of Co and Ni in hydrotreating reactions.

8. Conclusions

This contribution reports a theoretical investigation of hydrogen adsorption on Mo-based sulfide catalysts. The main results may be summarized as follows. At working conditions of these catalysts, on the stable Mo−S surface, only six-fold coordinated Mo cations are present. Substitution by Co or Ni leads to the creation of stable CUS sites on the working conditions of these catalysts. On the MoS_2 surface, hydrogen presents a high activation barrier, and the resulting dissociated species are metastable. On CoMoS surfaces, the ability to dissociate H_2 is dependent on the nature of the metal atom and the sulfur coordination environment. As an adsorption center, Co strongly favors molecular hydrogen activation as compared to Mo atoms. As a ligand of S atoms, Co increases their basicity. As a result, CoMoS surfaces present Co−S sites for which the dissociation is exothermic and weakly activated, hence demonstrating the crucial role of Co−S pairs in hydrogen activation over CoMo catalysts. On Ni−Mo−S surfaces, Ni−S pairs are not stable and do not provide an efficient way for hydrogen activation. Finally, these theoretical results are in good agreement with the recent experimental studies of H_2-D_2 exchange reactions, showing again the validity of this theoretical approach that provides a realistic description of these catalytic systems.

Acknowledgment. The authors thank Prof. G. Pérot from LACCO, France, for fruitful discussions. This work has been performed within the "GdR Dynamique Moléculaire Quantique Appliquée à la Catalyse", a joint project of Centre National de la Recherche Scientifique (CNRS), Institut Français du Pétrole (IFP), TOTAL FINA ELF, Universität Wien, and Technische Universiteit Eindhoven. Computational resources were provided by Dutch Computing Facilities (NCF) and the Centre de Ressources Informatiques de l'Université de Lille (CRI-USTL).

Supporting Information Available: Comparative study of supercells and discussion of calculation parameters affecting surface structures and energies (PDF). Typical output file (279 ko), showing calculation parameters and convergence for structure **2g**. This material is available free of charge via the Internet at http://pubs.acs.org.

JA011634O